Electronic Supporting Information

A facile one-pot method for synthesis of low-cost iron oxide/activated carbon nanotube electrode materials for lithium-ion batteries

Jie Ma[a], Fei Yu[a,b]*, Zhenhai Wen[c], Mingxuan Yang[a], Huiming Zhou[a], Cheng Li[a], Lu Jin [a], Lu Zhou[a], Lu Chen[a], Junhong Chen[a,c]*

[a] State Key Laboratory of Pollution Control and Resource Reuse, School of Environmental Science and Engineering, Tongji University, 1239 Siping Road, Shanghai 200092(P.R. China)

[b] School of Environmental Science and Engineering, Shanghai Jiao Tong University, 800 Dong Chuan Road, Shanghai 200240(P.R. China).

[c] Department of Mechanical Engineering, University of Wisconsin–Milwaukee, Milwaukee, WI 53211(USA)

Experiment

Preparation of IO/ACNT composites.

The IO/ACNT composites were prepared by a facile alkali-activated method using APCNTs. APCNTs samples were prepared by the catalytic chemical vapor deposition method[1]. In a typical preparation, the weight ratio of KOH to APCNTs was 1:1, and the APCNTs and KOH powders was mixed for 10 min using a mortar, which resulted in a uniform powder mixture. The mixture of APCNTs and KOH powders was placed in a stainless steel vessel, and then heated to 1,023 K for 1 h under flowing argon in a horizontal tube furnace, washed in the deionized water, and then dried.

Characterization methods

The microstructure and morphology of the IO/ACNT composites were analyzed using high resolution transmission electron microscopy (HRTEM, JEOL 2100F, Japan). The chemical composition of IO/ACNT hybrids was analyzed using the equipped energy-dispersive X-ray spectrometer (EDX). X-ray diffraction (XRD) experiments were conducted on specimens of the magnetic hybrid materials, and the X-ray diffractometer (Bruker D8 Advance, Bruker AXS, Germany) was operated at 40 KV and 40 mA. Nickel-filtered Cu $_{Ka}$ radiation was used in the incident beam. The specific surface area, pore volume and pore size distribution of the IO/ACNT composites were calculated from the adsorption/desorption isotherms of N_2 at 77 K by multi-point BET and DFT method using an Autosorb-iQ-C (Quantachrome, American, Inc.). And the sample was degassed at 373 K for 4 h prior to the measurements. X-ray photoelectron spectroscopy (XPS) analysis was carried out in a Kratos Axis Ultra DLD spectrometer, using monochromated Al Ka X-rays, at a base pressure of 1×10^{-9} Torr. Survey scans determined between 1,100 and 0 eV revealed the overall elemental composition of the sample and regional scans for specific elements were performed. The peak energies were calibrated by placing the

major C_{1s} peak at 284.6 eV. Samples were prepared identically to those of the batch experiments. Raman spectroscopy (JOBIN-YVON T64000) was used to further characterize APCNTs and IO/ACNT. TA Instruments® Q600 SDT thermal analyzer was used for high resolution thermogravimetric analysis (TGA) and differential thermal analysis (DTA). TGA and DTA curves were obtained by heating approximately 10 mg of fine samples from 50 to 900 °C at a heating rate of 10 °C/min in air.

Electrochemical Measurements

The working electrode was prepared by adding active materials (IO/ACNTs, 80%), acetylene black (10%), and poly vinylidene fluoride (binder, 10%) in 1-methyl-2-pyrrolidinone solution. After mixing uniformly, the mixture was then casted onto the copper foil current collector with the assistance of a doctor blade. It was noted that we herein used a high ratio of PVDF to achieve a tight binding of the active materials on the copper foil. The pellets were dried in vacuum at 120 ºC for 10 h, and then assembled into a half-battery with lithium pellet as reference electrodes in an Ar-filled glove box. The electrolyte solution was 1 M LiPF6 dissolved in a mixture of ethylene carbonate (EC), dimethyl carbonate (DMC) with the volume ratio of EC: DMC =1:1. Galvanostatic charging-discharging experiments were conducted to measure the capacity, rate capability and cycling stability using a Maccor battery tester system at room temperature. Discharge–charge curves were recorded at various current densities of 50-2,000 mA g^{-1} in the fixed voltage range of 2.5-0.005 V at room temperature.

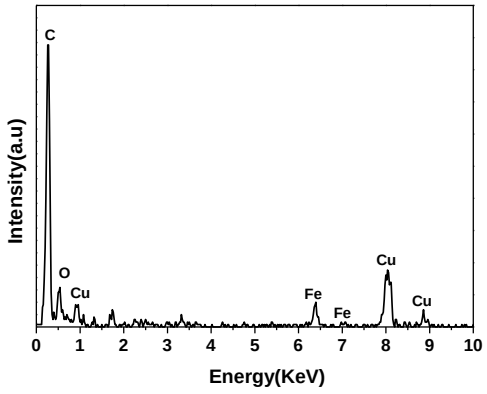

Fig. S1 Energy-dispersive X-ray spectrum of IO/ACNTs.

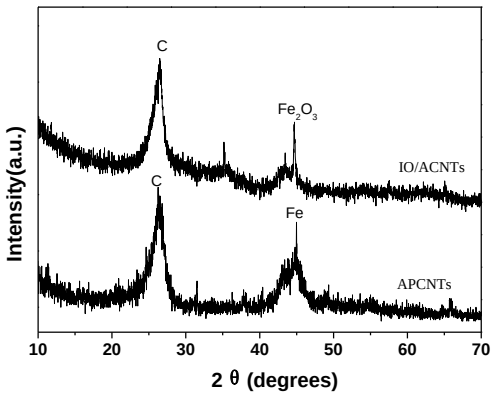

Fig. S2 the XRD curve of APCNTs and IO/ACNTs.

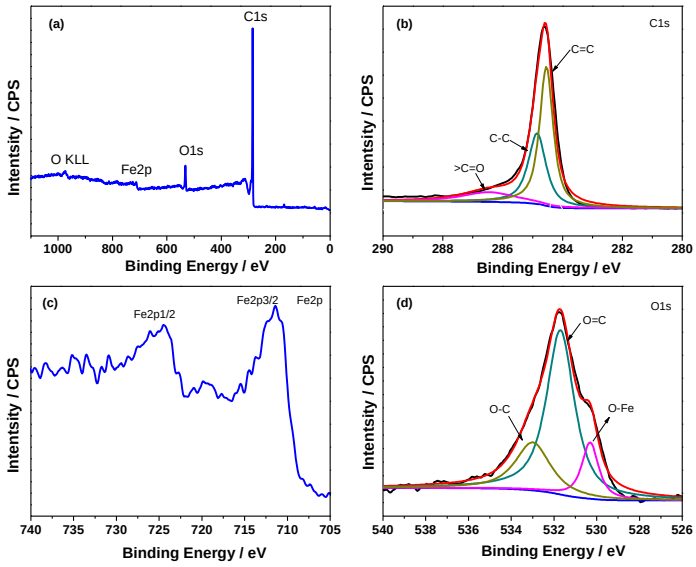

Fig. S3 XPS survey scans of the IO/ACNTs (a), the C1s deconvolution of IO/ACNTs (b), the Fe2p region of IO/ACNTs (c), and the O1s deconvolution of IO/ACNTs (d).

The composition of IO/ACNTs was further determined by XPS as shown in Fig. S3. Typical XPS survey scans of the IO/ACNTs are shown in Fig. S3a. Fig. S3b is the principal deconvoluted component of the C_{1s} region recorded for the IO/ACNTs. We can see that the strongest peak at 284.6 eV is assigned to double bonding carbons for CNTs resulting from non-functionalized carbon. The peak at the binding energy of about 285.1 eV is a consequence of single bonding carbon for CNTs[2]. The O_{1s} spectra consist of three peaks that are assigned to Fe-O (530.7 eV), C=O (531.7 eV) and C-O (533.0 eV) bonds [3], which suggests the introduction of new functional groups and iron oxide nanoparticles loading on the surfaces of IO/ACNTs. The Fe_{2p} spectrum (Fig. S3c) shows two broad peaks with satellite peaks at 711.4 eV and 724.5 eV representing

$Fe_{2p3/2}$ and $Fe_{2p1/2}$, respectively. The presence of these chemical bonds demonstrated that iron oxide nanoparticles were formed on the surface of IO/ACNTs.

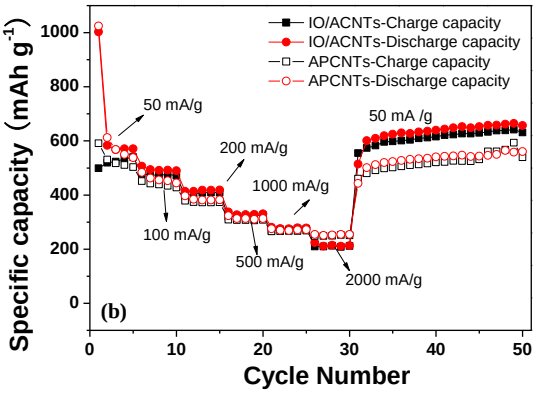

Fig. S4 Rate capability of the APCNTs and IO/ACNTs hybrids at the current densities between 50 and 2,000 mA g^{-1}.

Table S1 Specific surface area, pore volume, average pore size (BJH) of APCNTs and IO/ACNTs

Sample	BET area	Pore volume	Average pore size	Micropore	Mesopore	Macropore
	m^2/g	cc/g	nm	cc/g	cc/g	cc/g
APCNTs	113.5	2.004	11.03	0.048	0.305	1.651
IO/ACNTs	241.3	0.991	6.69	0.103	0.484	0.404

Reference:

1. J. Ma, J. N. Wang and X. X. Wang, *J Mater Chem*, 2009, **19**, 3033-3041.
2. C. C. Chen, C. F. Chen, C. M. Chen and F. T. Chuang, *Electrochem Commun*, 2007, **9**, 159-163.
3. P. C. J. Graat and M. A. J. Somers, *Appl Surf Sci*, 1996, **100**, 36-40.